Journal of Solid State Chemistry **149,** 284–291 (2000)
doi:10.1006/jssc.1999.8528, available online at http://www.idealibrary.com on IDEAL®

Luminescent Properties of Silver(I) Diphosphate of Compositions $Na_{2-x}Ag_xZnP_2O_7$

I. Belharouak,* C. Parent, P. Gravereau,* J. P. Chaminade,* G. Le Flem,* and B. Moine†

*ICMCB, UPR CNRS 9048, Avenue du Dr. A. Schweitzer, 33608 Pessac Cedex, France; and †Laboratorie de Physicochimie des Matériaux Luminescents, Université Claude Bernard, 43 Boulevard du 11 Novembre 1918, 69622 Villeurbanne Cedex, France

Received May 18, 1999; in revised form September 15, 1999; accepted October 11, 1999

The luminescence of silver(I) ions was investigated in diphosphate of compositions $Na_{2-x}Ag_xZnP_2O_7$. The $[P_2O_7]$ groups share corners with $[ZnO_4]$ tetrahedra in a layer arrangement. The Na/Ag atoms are located between layers in distorted oxygenated cubic sites sharing faces—with short intermetallic distances—or edges. Two luminescent centers were detected and attributed, respectively, to single Ag^+ and Ag^+–Ag^+ pairs. The luminescent parameters are discussed with respect to the symmetry of the silver sites and of the ionocovalent character of the silver oxygen bonds © 2000 Academic Press

Key Words: **diphosphate; rietveld; luminescence; silver; pairs.**

INTRODUCTION

The Ag^+ ion has a $4d^{10}$ outer electronic configuration. The fluorescence of this ion under UV excitation is due to the $4d^9 5s \leftrightarrow 4d^{10}$ transitions, strictly forbidden for the free ion but partially allowed in crystals through a coupling with lattice vibrations of odd parity. The $4d^{10}$ electronic configuration affects profoundly the Ag^+ crystal chemistry with a tendency for cluster formation. The structural aspect of the Ag^+ aggregation was discussed in a review (1). In most cases the crystal structure gives evidence of extended silver aggregates, where the Ag^+–Ag^+ distances can be less than the interatomic distance in silver metal, 289 pm.

The spectral properties of silver pairs are different from those of single Ag^+ ions, the emissions of which appearing, respectively, in the UV-visible and in the UV range. Therefore such luminescences can be observed only in colorless crystals, i.e., for compounds involving Ag–O ionic bonds (2). Such a requirement is fulfilled in phosphates in which the strong covalency of the P–O bond induces a ionic character of the opposite silver–oxygen bond. The covalent character of the anionic entities is emphasized in layer-like structures in which phosphate groups are located in two-dimensional sublattices. Such an atomic arrangement is typical of alkali diphosphates, e.g., KYP_2O_7 (3), $Na_2ZnP_2O_7$ (4), and $Na_2CoP_2O_7$ (blue form) (5), in which more or less alkali ion can be possibly replaced by Ag^+. In this context, the object of the present investigation is an analysis of the relationship between the structure and the luminescent properties of compounds of the general formula $Na_{2-x}Ag_xZnP_2O_7$ ($0 < x \leq 1$). We report successively the synthesis of the mixed silver sodium diphosphates, the growth of crystals with low silver concentration, the comparison between the crystal structures of $Na_2ZnP_2O_7$ and $Ag_2ZnP_2O_7$, and the identification and characteristics of the silver luminescent centers.

EXPERIMENTAL

The $Na_{2-x}Ag_xZnP_2O_7$ compounds were prepared by solid-state reaction from stoichiometric mixtures of Na_2CO_3, $AgNO_3$, ZnO, and $NH_4H_2PO_4$. The reagents were carefully mixed and progressively heated to 300°C to allow both ammonia and nitrous vapors to evolve. The obtained mixtures were finally heated at 720°C ($Na_2ZnP_2O_7$) and 450°C ($Ag_2ZnP_2O_7$) for 36 h. The obtained powders were white. The host $Na_2ZnP_2O_7$ melted congruently at 796°C. Small single crystals of this phase were grown from samples melted at 850°C and slowly cooled (3°C h^{-1}) to room temperature.

A large single crystal of $Na_{1.95}Ag_{0.05}ZnP_2O_7$ silver diphosphate composition was prepared using the Czochralski method (Fig. 1). The crystal growth was carried out under the following conditions. The 50-mm-diameter Pt crucible was inductively heated in air. The temperature of the melt was kept at a constant temperature of 805°C. A seed orientated along the [001] direction was rotated and withdrawn by motor drive at a speed of 10–20 rpm and 0.5–1 mm/h typically. The choice of the seed orientation will be explained in the next paragraph. Under these conditions a colorless crystal of about 15 mm diameter and 70 mm length was grown.

The emission and excitation spectra were recorded with a SPEX FLUOROLOG 212 I fluorimeter. The emission lifetime measurement was performed using as the excitation

0022-4596/00 $35.00

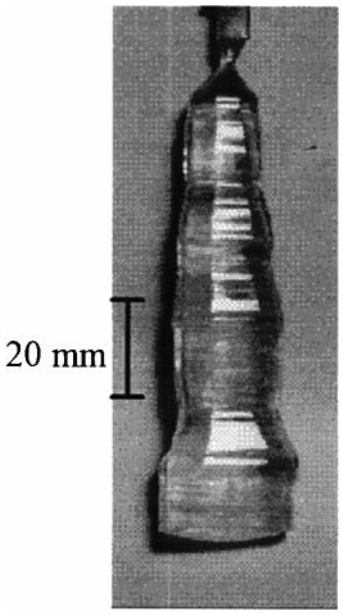

FIG. 1. Single crystal $Na_{2-x}Ag_xZnP_2O_7$:Ag^+ ($x = 0.05$) prepared using the Czochralski method.

source a dye laser beam (TDL IV model from QUANTEL) pumped by the second harmonic of a Q-switched Nd^{3+}: YAG laser. The second harmonic of the dye laser allows excitation at 310 nm. A mixture of this second harmonic with the 1060 nm YAG emission in a nonlinear crystal generates excitation at 240 nm. The emission was dispersed by a HILGER computer scannable monochromator, detected with a HAMAMATSU R 1477 PMT, and recorded using a multichannel analyzer (STANDFORD INSTRUMENT SR 430) with a minimum dwell time per channel of 5 ns.

STRUCTURAL INVESTIGATION

The powder diffraction pattern of $Na_2ZnP_2O_7$ can be indexed assuming a tetragonal unit cell. The experimental specific mass 3.115 g cm^{-3} is close to the value calculated from X-ray data, 3.127 g cm^{-3}. The parameters $a =$ 768.5 pm, $c = 1026.5$ pm are close to those previously reported by Majling *et al.* (6), $a = 769.2$, $c = 1027.3$ pm, and the crystal structure was previously described by Erragh *et al.* (4) on the basis of the parameters $a = 765.6$ and $c = 1023.3$ pm. A close examination of the Weissenberg and Burger photographs reveals a system of strong reflections consistent with the previous unit cell and a system of additional weak reflections which involves a new cell of a' and c' parameters such as $a' = 2\sqrt{2}\cdot a$, and $c' = c$. This will be reported on in a parallel publication (7). Fig. 2 compares (001) projections of both models. Basically the structure is typical of a layered arrangement. Within a layer each $[ZnO_4]$ tetrahedron shares its four corners with different $[P_2O_7]$ groups. The sodium atoms are located between the layers in distorted eightfold coordinated sites. The sodium sites are connected through common faces, which involves short sodium–sodium distances (305 pm), or through common edges, giving rise to longer sodium–sodium distances (360 and 450 pm). In the (a', c') model the position of the phosphorus, zinc, and oxygen atoms are slightly shifted every other layer. Therefore, the simplified model with the (a, c) parameters can be usefully considered to analyze the structural evolution of the $Na_{2-x}Ag_xZnP_2O_7$ compounds and, accordingly, the effect of composition on the luminescent properties. The substitution of silver for sodium induces a significant increase of parameter c (Fig. 3). Effectively, the replacement of the Na^+ ion by Ag^+ with a greater ionic radius induces the expansion of the crystalline cell mainly by increasing the interlayer distance. The refinement of the structure of $Ag_2ZnP_2O_7$ was carried out on powder samples using the Rietveld profile analysis to the X-ray diffraction diagram. The starting structural hypothesis was the (a, c) model first adopted for $Na_2ZnP_2O_7$. The structural hypothesis based on the (a', c') model was attempted but excluded since it involves more than 200 refinement parameters. The experimental conditions of the data collection are given in Table 1. Final coordinates and selected atomic distances

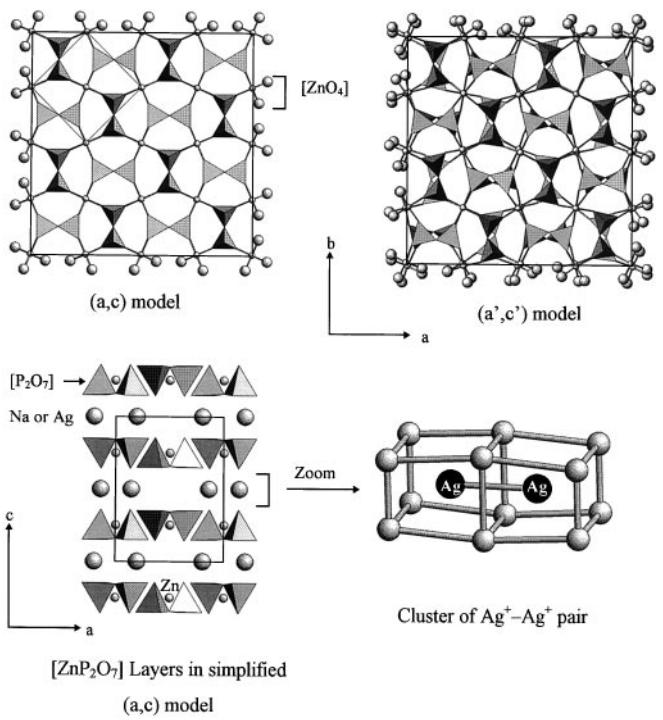

FIG. 2. Projections of the (a, c) and (a', c') models of $Na_2ZnP_2O_7$ diphosphate.

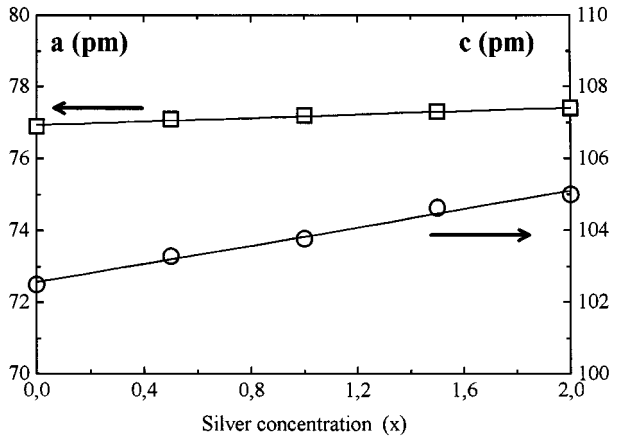

FIG. 3. Evolution of cell parameters in polycrystalline $Na_{2-x}Ag_xZnP_2O_7$ as a function of silver concentration.

and angles are listed in Tables 2 and 3. Figure 4 compares the experimental and calculated X-ray diffraction patterns.

The P–O distances in the $[P_2O_7]$ groups are typical of a diphosphate entity in which the longer distance (158.3 pm) characterizes P–O–P bridge. The $[ZnO_4]$ tetrahedron is almost regular, with a Zn–O distance (193 pm) consistent with the table of Shannon ($d_{Zn-O} = 200$ pm) (8). In α- and β-$AgZnPO_4$ the Zn–O distances are included between 189 and 195 pm (9). The coordination number of the different silver atoms is 8, and the silver oxygen distances are in accordance with those previously reported for several silver phosphates (Table 4).

The silver oxygenated sites are connected through common faces (Ag(1)–Ag(1)) or common edges (Ag(1)–Ag(2) and Ag(2)–Ag(2)). The respective Ag–Ag distances are 308.8, 366, and 431.4 pm. Such short distances between the Ag(1) positions have been observed previously in several phosphates, e.g., in Ag_3PO_4 ($d_{Ag-Ag} = 301.3$ pm) (10), $AgCuPO_4$ ($d_{Ag-Ag} = 306.7$ pm) (11), and $AgPO_3$ ($d_{Ag-Ag} = 315$ pm) (12).

TABLE 1
Details of Rietveld Refinement for $Ag_2ZnP_2O_7$

Crystallographic data	
Symmetry	tetragonal
Space group	$P4_2/mnm$
Z	4
Cell parameters	$a = 774.3$ (2) pm
	$c = 1050.0$ (4) pm
Volume	629.2 (3) × 10^6 pm^3
Data acquisition	
Radiation	Cu$K\alpha$ ($\lambda = 156.18$ pm)
Angular range	$10° < 2\theta < 120°$
Step scan increment (°2θ)	0.02°
Counting time by step	30 s
Refinement conditions	
Program	FULLPROF (20)
Number of reflections	282
Number of refined parameters	35
Pseudo-Voigt function	P.V. = $\eta L + (1-\eta)G$)
	$\eta = 0.845$ (5)
Caglioti law parameters	$U = 0.292$ (5)
	$V = -0.105$ (9)
	$W = 0.037$ (4)
Asymmetry factors	0.069 (8) and 0.005 (6)
R_F	0.048
R_B	0.051
R_p	0.093
R_{wp}	0.108
cR_p	0.115
cR_{wp}	0.126
χ^2	3.75

TABLE 2
Final Atomic Coordinates and Isotropic Temperature Factors (with Standard Deviations in Brackets) for $Ag_2ZnP_2O_7$

Atoms	Positions	x	y	z	B_{iso} (Å^2)
Zn	4*d*	0	0.5	0.25	1.26 (4)
Ag1	4*f*	0.359 (4)	0.359 (4)	0	2.31 (5)
Ag2	4*g*	0.303 (1)	0.303 (1)	0.5	2.26 (5)
P	8*j*	0.135 (3)	0.135 (3)	0.211 (2)	1.05 (7)
O1	4*e*	0	0	0.157 (3)	1.97 (6)
O2	8*j*	0.126 (5)	0.126 (5)	0.356 (2)	1.24 (5)
O3	16*k*	0.086 (1)	0.306 (3)	0.154 (4)	1.75 (4)

LUMINESCENCE INVESTIGATION

1. Luminescence Spectra of the Compound $Na_{1.95}Ag_{0.05}ZnP_2O_7$

This composition was selected as a model system for low activator concentration. In Fig. 5 the emission spectrum under U.V. excitation is shown ($\lambda_{exc.} = 230$ and 280 nm). At room temperature two broad band emissions are observed, one in the UV range, peaking at 317 nm and labeled (A), and one at lower energy, with a maximum appearing about 390 nm and labeled (C). No additional emissions were

TABLE 3
Selected Interatomic Distances (pm) and Angles (°) for $Ag_2ZnP_2O_7$

P–O1	158.3 (2)		
P–O2	152.6 (3)		
P–O3	2 × 150.2 (3)	Zn–O3	4 × 193 (1)
P–O1–P (°)	138.6 (5)		
Ag1–O2	4 × 256.4 (4)	Closest silver–silver distances	
Ag1–O3	4 × 269.3 (4)	Ag(1)–Ag(1)	308.8
Ag2–O1	2 × 271.5 (2)	Ag(1)–Ag(2)	365.9
Ag2–O2	2 × 245.8 (3)	Ag(2)–Ag(2)	431.4
Ag2–O3	4 × 285.1 (5)		

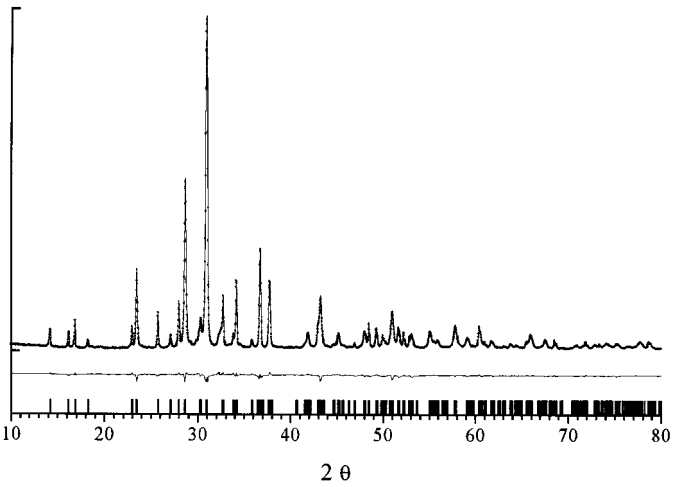

FIG. 4. The observed (dots), calculated (solid line), and difference XRD profiles with Rietveld refinement of $Ag_2ZnP_2O_7$.

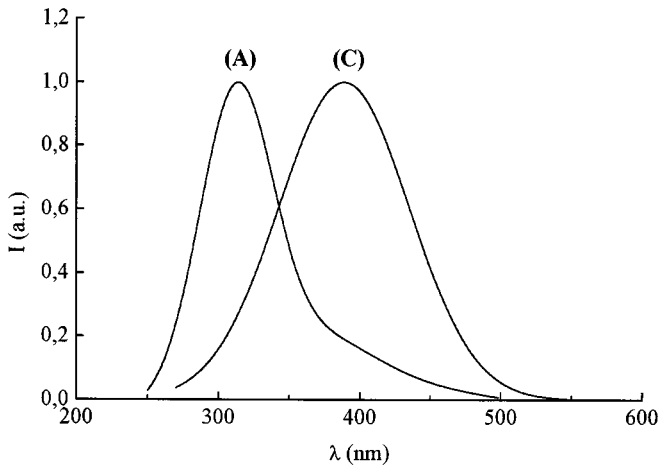

FIG. 5. Emission spectra of the Ag^+ luminescence in crystalline $Na_{1.95}Ag_{0.05}ZnP_2O_7$ for 230 nm (emission (A)) and 280 nm (emission (C)) excitations at 300 K.

observed at 6 K. The excitation spectrum of the (A) emission shows two broad bands peaking, respectively, at 205 nm (I) and 222 nm (II) (Fig. 6a). The excitation spectrum of the (C) emission exhibits a weak and broad band around 260 nm in addition to the excitation bands for the (A) emission (Fig. 6b). Such spectral distribution suggests an (A) → (C) energy transfer. This transfer is illustrated by the small overlapping between the (A) emission and the (C) excitation band (Fig. 7). (A) and (C) can be considered, respectively, as donor and acceptor centers. Table 5 summarizes these results and reports the Stokes shifts of both luminescent centers.

2. *Effects of Silver Concentration and Temperature on the Emission Intensities*

At room temperature the intensity of the (A) emission increases in the range of composition $0 < x \leq \sim 0.2$ and then decreases and is quenched for $x \approx 0.6$. The (C) center can be detected between $x \approx 0.005$ and $x \approx 1.25$, with a maximum intensity for the compound $x \approx 0.6$ (Fig. 8a).

The intensities of the (A) and (C) emissions decrease between 4 and 150 K and then are independent of the temperature effect (Fig. 8b).

TABLE 4
Coordination of Ag^+ in Several Phosphates

Phosphate composition	*d*Ag–O (pm) Min.	*d*Ag–O (pm) Max.	Silver coordination number	Ref.
$AgZr_2(PO_4)_3$	256	256	6	(19)
$AgPO_3$	237	270	5	(12)
$AgMg(PO_3)_3$	234	272	6	(21)
$AgBa(PO_3)_3$	231	264	6	(21)
$Ag_2H_2P_2O_7$	244	251	6	(22)
α-$AgZnPO_4$	235	317	6&8	(9)
β-$AgZnPO_4$	235	317	6&9	(9)
$AgBePO_4$	260	313	7&12	(9)
$Ag_2ZnP_2O_7$	240	288	8	this work

3. *Luminescence Dynamics*

The decay time τ of both luminescences was measured as a function of temperature between 4 and 300 K under 230 nm excitation. The decays are single exponentials in the whole temperature range. Figure 9 gives the temperature dependence of τ for the (A) fluorescence. At 4 K, τ is approximately 38 μs and then decreases between 5 and 100 K before reaching an almost constant value ($\tau \approx 25$ μs) at higher temperature. This temperature dependence is typical of a three-level system, which is described by the rate equation

$$\frac{1}{\tau} = \frac{A_{31} + A_{21}\exp(-\varepsilon/KT)}{1 + \exp(-\varepsilon/KT)}, \qquad [1]$$

where A_{21} and A_{31} are the radiative transition probabilities between the excited states (upper level 2 and lower level 3) and the ground state and ε represents the energy mismatch between the two excited states. Table 6 collects the best parameters obtained after a fit of the experimental data, using this rate equation.

Figure 9 also gives the temperature dependence of τ for the (C) fluorescence. The curve can be divided into three parts. At low temperature, between 6 and 30 K, τ increases; then the lifetime decreases slowly up to 100 K. Above this temperature the lifetime decreases more abruptly in relation

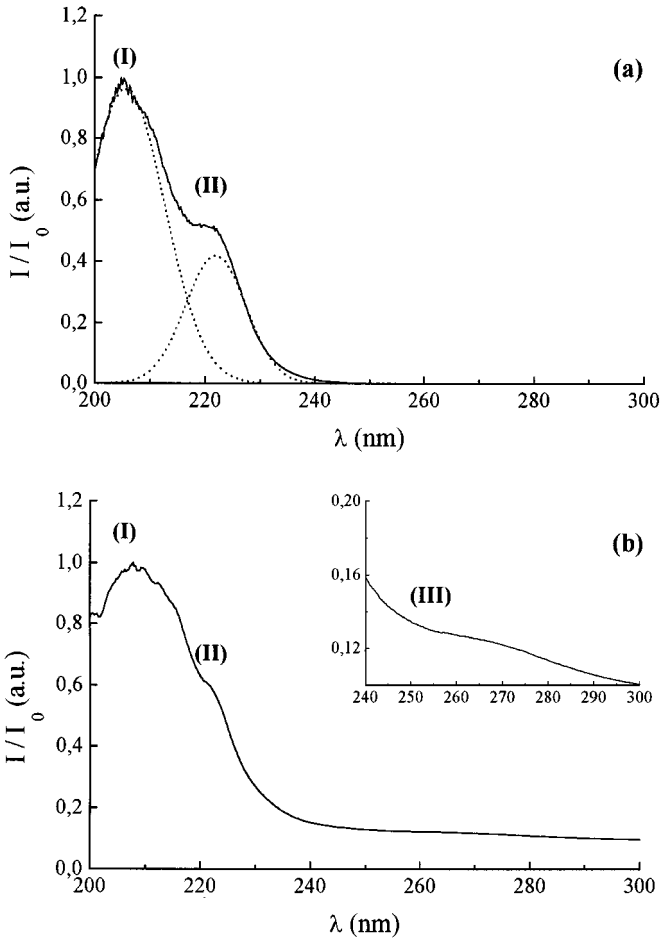

FIG. 6. Excitation spectra for the emissions detected in crystalline $Na_{1.95}Ag_{0.05}ZnP_2O_7$. The emission wavelengths for the excitation spectra are 317 nm (emission A) (a) and 450 nm (emission C) (b). ($T = 300$ K.)

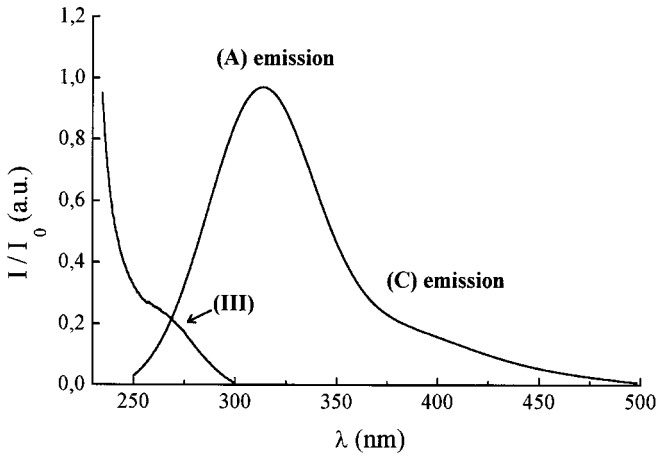

FIG. 7. Overlapping between the (A) emission and the (C) excitation (band III) at 300 K.

to probable thermal quenching of the luminescence. The fitting of the curve between 6 and 55 K necessitates the introduction of an additional excited state as suggested previously by Boutinaud *et al.* (13). This four-level model (ground state + three excited emitting levels) can be written as

$$\frac{1}{\tau} = \frac{A_{21} + A_{31}\exp(-\varepsilon_{32}/KT) + 2A_{41}\exp(-\varepsilon_{42}/KT)}{1 + \exp(\varepsilon_{32}/KT) + 2\exp(\varepsilon_{42}/KT)}.$$

The calculated parameters, which have the same signification as in Eq. [1], and the corresponding energy diagram are given in Table 6 and Fig. 9.

DISCUSSION

1. Crystal Chemistry of Silver Zinc Phosphates

Basically, the crystal chemistry of the silver phosphates is remarkable for its large distribution of silver oxygen distances and for its various coordination numbers at the silver sites. These two trends emerge from the data collected in Table 4. The modulation of the silver–oxygen bond covalence can be qualitatively deduced from detailed examination of the crystal structure. In this context the atomic arrangements of three silver zinc phosphates can be usefully compared, the polyphosphate $AgZn(PO_3)_3$ (14), the α an β forms of the monophosphate $AgZnPO_4$ (9), and the diphosphate $Ag_2ZnP_2O_7$. The structure of these phosphates can be described as made up of a covalent oxygenated framework in which the silver atoms are located. In the polyphosphate, infinite $(PO_3)_\infty$ chains are found running in zig–zag configuration, leading to a one-dimensional structural type. The zinc and silver atoms are located, respectively, in slightly distorted octahedra and in antiprisms sharing faces giving rise to infinite chains running along one crystallographic direction. The silver oxygen distances are between 232 and 272 pm. In this case the zinc atoms do not belong to the covalent framework.

The structure of the two forms of the monophosphate is silica-like, consisting of a $[ZnPO_4]$ tetrahedral three-dimensional framework with cavities filled by the silver atoms. The silver–oxygen distance distribution is rather large, between 235 and 317 pm. The structural characters of the investigated diphosphate are intermediate. The covalent

TABLE 5
Luminescence Data of the (A) and (C) Centers in $Na_{1.95}Ag_{0.05}ZnP_2O_7$

Emissions	$\lambda_{em.} \pm 0.5$ (nm)	$\lambda_{exc.} \pm 0.5$ (nm)	Stokes shift (cm^{-1})
(A)	205, 222	317	13,500
(C)	205, 222, and 260	390	12,800

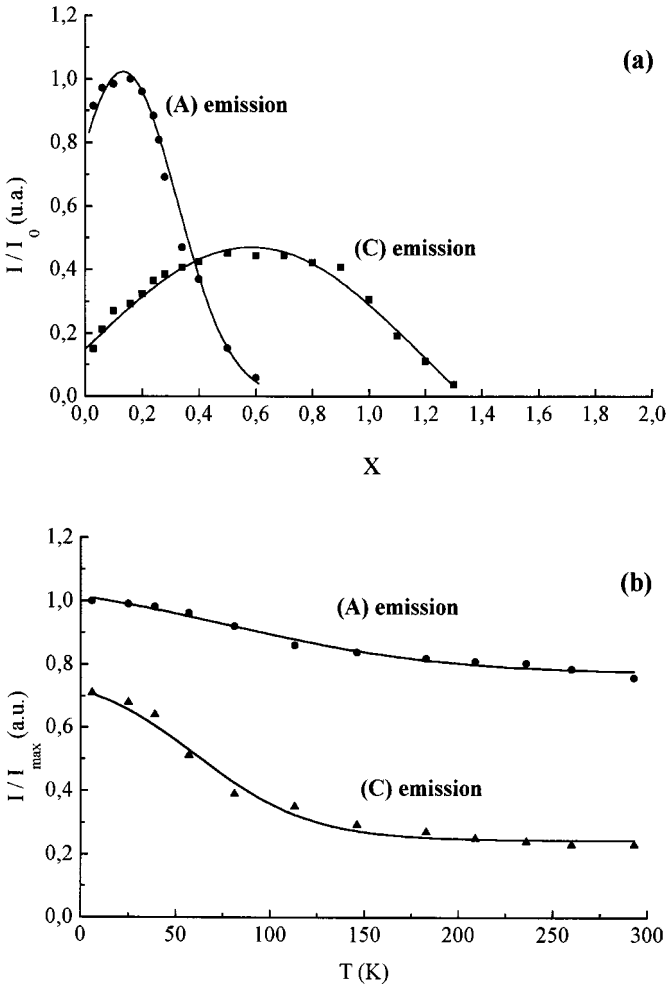

FIG. 8. (a) Evolution of the relative intensities of (A) ($\lambda_{exc.} = 230$ nm) and (C) ($\lambda_{exc.} = 280$ nm) emissions as a function of silver concentration for polycrystalline $Na_{1-x}Ag_xZnP_2O_7$ at 300 K. (b) Temperature dependence of the relative intensity of the (A) and (C) emissions for the $Na_{1.95}Ag_{0.05}ZnP_2O_7$ crystal.

framework is two-dimensional and implies also the zinc ions. The dispersion of the silver oxygen distances is found to be between that observed for the polyphosphate and that observed for the monophosphate ($240 < d < 288$ pm). Two additional structural features must be exphasized, the rather unusual coordination number of both silver sites, 8, which corresponds to distorted cubes, and the appearance of one short silver–silver distance of 309 pm.

The large coordination number and silver oxygen distances allow us to conclude that the silver–oxygen bond in the investigated diphosphate has a strongly ionic character, which explains the white color of the powder samples (2) and is consistent with the analysis of the luminescent properties as resulting from ionic silver centers.

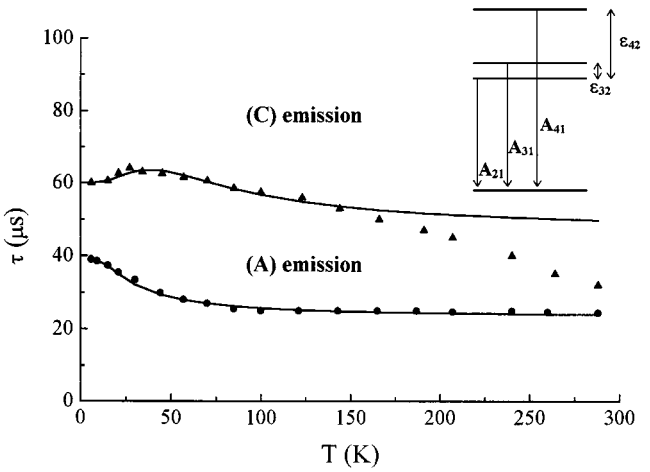

FIG. 9. Temperature dependence of the decay time of the (A) and (C) emissions for the $Na_{1.95}Ag_{0.05}ZnP_2O_7$ crystal. (Insert) Scheme of the four-level system with fitting parameters.

2. *Origin of the Luminescent Properties*

As mentioned in the Introduction, the luminescence of Ag^+ has been studied in alkali halide crystals (15,16) and in alkali-earth halides (17). In sodium, chloride-like crystals Ag^+ substitutes for the cation without any need for charge compensation, which is the case in the investigated phosphate. On the other hand, the local symmetry for Ag^+ in fluorite-type structures is cubic, i.e., very close to the silver environment in the diphosphate. These reference systems exhibit only one UV luminescence for low silver concentration, and additional emission bands can appear as the silver concentration increases. The excitation and emission spectra involve $4d^{10} \leftrightarrow 4d^9 5s$ transitions. The energy of the $4d^9 5s$ states is dependent on the spin orbit coupling and the crystal field effects.

Table 7 compares the parameters of the (A) luminescence with those of various halogenides and phosphates in which the silver ions are isolated. This comparison allows us to ascribe the (A) emission to single Ag^+. Even at low temperature two different (A) emissions potentially originated from the Ag(1) or Ag(2) crystallographic centers cannot be

TABLE 6
Fitting Parameters of the Thermal Evolution of the Emission Decays for the (A) and (C) Centers

Emission decay of the (A) center ($\lambda_{em.} = 315$ nm), three-level system parameters			Emission decay of the (C) center ($\lambda_{em.} = 390$ nm), four-level system parameters				
A_{21} (s^{1-})	A_{31} (s^{1-})	ε (cm^{-1})	A_{21} (s^{1-})	A_{31} (s^{1-})	A_{41} (s^{1-})	ε_{32} (cm^{-1})	ε_{42} (cm^{-1})
60,975	25,640	36	7,800	31,250	16,660	40	105

TABLE 7
Luminescence Data of Isolated Ag^+ Centers in Various Host Lattices (SS Stands for Stokes Shift)

Compounds	$\lambda_{em.}$ (nm)	$\lambda_{exc.}$ (nm)	SS (cm^{-1})	A_{21} (s^{-1})	A_{31} (s^{-1})	ε (cm^{-1})	Ref.
NaCI:Ag^+	244	117	—	40000	2700	59	(23)
KCI:Ag^+	274	180	—	100000	12500	35	(23)
SrF_2:Ag^+	314	227	12200	112000	7763		(13)
SrB_4O_7:Ag^+	288	245	6200	142900	28600	50	(24)
$AgMg(PO_3)_3$	317	225	12900	142000	48780	80	(21)
$AgZn(PO_3)_3$	325	225	13700	166667	40000	85	(21)
$AgBaP_3O_9$	365	250	12600				(21)
$Na_2ZnP_2O_7$:Ag^+	317	222	13500	60975	25000	36	this work

detected. The large Stokes shift is related to the perturbation of the excited states by the phosphate group's vibration. Isolated d^{10} ion luminescence is usually interpreted by use of a three-level system (18) to parametrize the temperature dependence of the lifetime emission. The results of the calculations (Eq. [1]) given in Table 7 confirm this hypothesis.

Such luminescences result basically from the location of silver atoms in off-center positions in their sites. For example, no luminescence was detected at room temperature in the nasicon-type phosphate $AgZr_2(PO_4)_3$, in which Ag^+ is located at the center of an oxygenated antiprism (19). Moreover, Ag^+ trapped in the octahedral sites of NaCl exhibits the lower emission probability. In addition to this symmetry argument, the calculated emission probability of the radiative emitting level A_{31} can be qualitatively related to the covalency of the silver ligand bond. This parameter is higher in oxides than in halogenides, in which the silver ligand bonds are more ionic. The coordination number at the silver site is higher for the borate (CN = 9) and the diphosphate (CN = 8) than for the polyphosphates (CN = 6), which involves more ionic silver oxygen bonds and can explain the corresponding lower A_{31} values. Actually the variation of A_{31} is rather sensitive to the influence of the silver local symmetry.

The unusual behavior of the (C) emission temperature dependence has been previously observed for one of the optical centers detected in SrF_2, Ag^+ (13). The associated center consists of two $[AgF_8]$ cubes joined by a common face. The geometry of the $[Ag_2F_{12}]^{10-}$ cluster involves a reduced Ag^+–Ag^+ distance of 290 pm. This geometric arrangement is almost identical to the structural association resulting from two Ag(1) nearest neighbors of the diphosphate (Fig. 2). In this cluster the silver–silver maximum distance ($x = 2$) is 309 pm. Therefore this second luminescence (C) can be ascribed to $(Ag^+)_2$ pairs. The energy mismatches ε_{32} and ε_{42} have the same order of magnitude as those calculated in SrF_2:Ag^+, but the emission probability of the emitting level A_{21} is higher for the phosphate ($7800\ s^{-1}$ vs $5000\ s^{-1}$ for the fluoride) due to the larger silver oxygen bond covalency.

The concentration quenching of the (A) emission (for $x > 0.6$) seems to be related to the parallel increase of the (C) emission and consequently results from the (A) → (C) energy transfer. The origin of the concentration quenching of the (C) emission may be partially explained by the two-dimensional distribution of the silver ions in the structure, which makes easier the energy diffusion to trapping defects.

CONCLUSION

The structure of $Na_{2-x}Ag_xZnP_2O_7$ can be described as made up of strongly covalent $[ZnP_2O_7]$ layers, in between which are located the monovalent cations Na^+/Ag^+. This structural arrangement induces a significant ionic character of the sodium/silver sites (CN = 8). Two luminescent centers, (A) and (C), emitting in the UV range ($\lambda_{em.} =$ 317 nm) and in the near-UV range ($\lambda_{em.} = 390$ nm) were attributed, respectively, to single Ag^+ and Ag^+–Ag^+ pairs. The thermal behavior of the lifetime of (A) is described assuming a three-level system, whereas a four-level scheme is needed to analyze the properties of the silver pairs. The relatively low probability of the single Ag^+ emission is consistent with the ionic character of the silver oxygen bonds. The dynamics of the (C) emission is governed by the site symmetry of the oxygenated cluster containing the silver pairs.

REFERENCES

1. M. Jansen, *Angew. Chem Int. Ed. Engl.* **26**(26), 1098 (1987).
2. H. Y. B. Hong, J. A. Kafalas, and J. B. Goodenough, *J. Solid State Chem.* **9,** 345 (1974).
3. A. Hamady, M. Fouzi Zid, and T. Jouini, *J. Solid State Chem.* **113,** 120 (1994).
4. F. Erragh, A. Boukhari, A. Sadel, and E. M. Holt, *Acta Crystallogr.* **C54,** 1376 (1998).
5. F. Erragh, A. Boukhari, B. Elouadi, and E. M. Holt, *J. Crystallogr. Spectrosc. Res.* **21**(23), 321 (1991).
6. J. Majling, S. Palco, F. Hanic, and J. Petrovic, *Chem. Zvesti* **28**(3), 294 (1974).
7. I. Belharouak, P. Gravereau, J. P. Chaminade, C. Parent, E. Le Brau, and G. Le Flem, submitted.
8. R. D. Shannon, *Acta Crystallogr. A* **32,** 751 (1976).
9. R. Hammond, J. Barbier, and C. Gallardo, *J. Solid State Chem.* **141,** 177 (1998).
10. H. N. Ng, C. Calvo, and R. Faggiani, *Acta Crystallogr. B* **24,** 1968 (1982).
11. M. Quarton and M. T. Oumba, *Mater. Res. Bull.* **18,** 967 (1983).
12. K. H. Jost, *Acta Crystallogr.* **14,** 779 (1961).
13. P. Boutinaud and H. Bill, *J. Phys. Chem. Solids* **57**(1), 55 (1996).
14. M. Averbuch-Pouchot and A. Durif, *J. Solid State Chem.* **49,** 341 (1983).
15. K. Fussganger, *Phys. Status Solidi* **34,** 157 (1969).

16. C. Pedrini, H. Chermette, A. B. Goldberg, D. S. McClure, and B. Moine, *Phys. Status Solidi B* **120,** 753 (1983).
17. P. Boutinaud, A. Monnier, and H. Bill, *J. Phys. Condens. Matter* **6,** 8931 (1994).
18. C. Pedrini, *J. Phys. Chem. Solids* **41,** 653 (1979).
19. H. Y. P. Hong, *Mater. Res. Bull.* **11,** 173 (1976).
20. J. Rodriguez-Carvajal, *in* "Powder Diffraction Satellite Meeting of the XVth Congress of IUCr, Toulouse, 1990," abstract, p. 127.
21. I. Belharouak, H. Aouad, M. Mesnaoui, M. Maazaz, C. Parent, B. Tanguy, P. Gravereau, and G. Le Flem, *J. Solid State Chem.* **145,** 97 (1999).
22. M. Averbuch-Pouchot and A. Durif, *Eur. J. Solid State Inorg. Chem.* **29,** 993 (1992).
23. B. Moine, Thesis, Université Claude-Bernard Lyon 1, Lyon, France, 1984.
24. A. Meijerink, M. M. E. van Heek, and G. Blasse, *J. Phys. Chem. Solids* **54**(8), 901 (1993).